Proceedings of the ASME 2010 3rd Joint US-European Fluids Engineering Summer Meeting and 8th International Conference on Nanochannels, Microchannels, and Minichannels
FEDSM-ICNMM2010
August 1-5, 2010, Montreal, Canada

FEDSM-ICNMM2010-30587

VARIABLE PROPERTY EFFECTS IN SIMULTANEOUSLY DEVELOPING GASEOUS SLIP-FLOW IN RECTANGULAR MICROCHANNELS WITH PRESCRIBED WALL HEAT FLUX

Azad Qazi Zade
University of Waterloo
Mechanical & Mechatronics Engineering
Waterloo, Ontario, Canada

Metin Renksizbulut
University of Waterloo
Mechanical & Mechatronics Engineering
Waterloo, Ontario, Canada

Jacob Friedman
Ryerson University
Mechanical & Industrial Engineering
Toronto, Ontario, Canada

ABSTRACT

The effects of variable physical properties on the flow and heat transfer characteristics of simultaneously developing slip-flow in rectangular microchannels with constant wall heat flux are numerically investigated. A co-located finite-volume method is used in order to solve the mass, momentum and energy equations in their most general form. Thermophysical properties of the flowing gas are functions of temperature, while density and Knudsen number are allowed to change with both pressure and temperature. Different Knudsen numbers are considered in order to study the effects of slip-flow. Simulations indicate that the constant physical property assumption can result in under/over-prediction of the local friction and heat transfer coefficients depending on the problem configuration. Density and thermophysical property variations have significant effects on predicting flow and heat transfer characteristics since the gas temperature constantly changes as a result of the applied wall heat flux. Heat transfer coefficient is affected both due to the change in the velocity field and change in thermophysical properties. Also temperature dependence of the local Knudsen number can significantly alter the friction coefficients due to its strong dependence on slip conditions. The degree of discrepancy varies for different cases depending on the Knudsen number, and the applied heat flux strength and direction (cooling versus heating).

INTRODUCTION

Micro-scale devices have gained significant popularity in recent years due to their desirability in various technical fields. As these devices become more and more sophisticated, there is a push towards smaller dimensions where the conventional theories associated with macro-scale devices begin to fail. A good example is the velocity slip effect in microfluidic devices where the no-slip assumption at the walls breaks down, and in the case of heat or mass transfer, a temperature-jump or a concentration-jump is observed between the surface and the adjacent fluid layer.

The Knudsen number Kn, defined as the ratio of molecular mean-free-path to the characteristic length scale of the problem, can be used to estimate the applicability of the continuum equations in dealing with problems that involve very small length scales or rarefied gases. For finite values of the Knudsen number, the continuum equations cannot be applied directly and either they should be modified or molecular models should be employed. In the case of rarefied gas flows, it is known that for $Kn < 0.001$ the continuum models are valid, and for $Kn > 10$, free-molecular models should be employed. In the mid range, neither continuum models nor free-molecular models are satisfactory and another classification is needed: slip-flow for the range $0.001 < Kn < 0.1$ and transition-flow for the range $0.1 < Kn < 10$ are considered to be appropriate descriptions [1]. In the slip-flow regime, the continuum equations can still be employed but proper velocity-slip and temperature-jump boundary conditions should be specified. Experimental, analytical and numerical studies have confirmed the applicability of the continuum equations along with proper slip/jump boundary conditions in the slip-flow range of Knudsen numbers [2-8].

Morini [9] conducted a comprehensive review of convective heat transfer in microchannels. He concluded that besides the disagreement between the friction factor and Nusselt number for micro-flows and the conventional macro-flow predictions, the reported flow and heat transfer characteristics of microchannels are inconsistent among different researchers. This discrepancy is attributed to a number of factors such as the surface conditions, rarefaction and compressibility, property variations and viscous heating effects.

Most of the available analytical and numerical investigations are limited to 2-D geometries with simplifying assumptions for different boundary conditions [10-14]. Flow and heat transfer characteristics of isoflux rectangular microchannels with slip/jump boundary conditions have also been studied. In reviewing the results of theoretical and experimental studies, Rostami et al. [15] concluded that the available conventional macro-channel theories are not adequate to predict the flow and heat transfer characteristics of gaseous flow in microchannels. Morini and Spiga analytically determined the velocity field in fully developed incompressible laminar slip-flow in rectangular microchannels of arbitrary aspect ratio [4]. Yu and Ameel [16] used an integral transform technique to solve the energy equation with no axial conduction assuming a fully developed incompressible slip-flow field with constant wall heat flux. Kuddusi and Ceten [17] conducted an analytical study on the heat transfer properties of hydrodynamically developed incompressible flow under different constant wall heat flux boundary condition combinations. Nonino et al. [18] studied the effect of temperature dependent viscosity on heat transfer characteristics of no-slip liquid flows with convective boundary condition. Their results suggest that the temperature dependence of viscosity cannot be neglected within a considerable range of working conditions especially in the channel inlet region. Van Rij et al. [19, 20] studied the effects of viscous dissipation and second order slip/jump boundary conditions on flow and heat transfer characteristics of rectangular microchannels. In order to avoid large changes in the physical properties, they chose a very small wall heat flux or temperature difference between the inlet and wall, and thus, employed constant physical properties in their simulations.

In the present work, three-dimensional gaseous slip-flow and heat transfer in rectangular microchannels of different aspect ratios are studied numerically for developing flow and temperature fields at different Knudsen numbers. The governing equations are in their most general form with all terms included. Also, the compressibility effect and variation of physical properties with temperature are included in the simulations.

MATHEMATICAL FORMULATION

A schematic view of the microchannel and the coordinate system is depicted in Figure 1. The aspect ratio of the channel is $\alpha = W/H$ with H and W being the channel height and width, respectively. The flow direction is along the x axis. For the low Peclet number values used in this study, a channel length of $6D_h$ is sufficient for the flow and temperature fields to develop [19], where $D_h = 2WH/(W+H)$ is the hydraulic diameter of the channel. Also, since the main scope of the present work is to examine the importance of property variations mainly due to temperature change, a relatively short microchannel is chosen for the simulations to avoid large pressure drops.

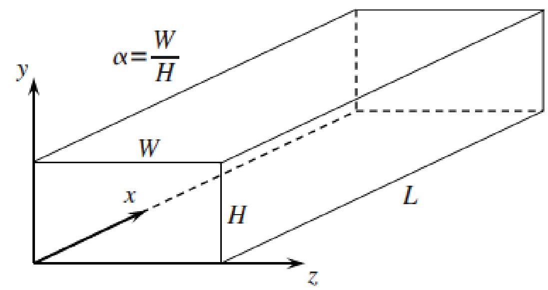

Figure 1: Schematic of physical domain and coordinate system

The steady-state compressible conservation equations can be expressed in non-dimensional form as:

$$\frac{\partial}{\partial x_i}(\rho u_i) = 0 \tag{1}$$

$$\rho u_i \frac{\partial u_i}{\partial x_j} = -\frac{\partial}{x_j}(p\delta_{ij}) + \frac{1}{Re}\frac{\partial}{x_j}\left[\mu\left(\frac{\partial u_i}{\partial x_j} + \frac{\partial u_j}{\partial x_i}\right) - \frac{2}{3}\mu\frac{\partial u_k}{\partial x_k}\delta_{ij}\right] \tag{2}$$

$$\rho c_p \frac{\partial}{\partial x_i}(u_i T) = (\gamma_0 - 1)Ma^2 \frac{\partial}{\partial x_i}(u_i p) + \frac{1}{RePr}\frac{\partial}{\partial x_i}\left(k\frac{\partial T}{\partial x_i}\right) + (\gamma_0 - 1)\frac{Ma^2}{Re}\left[\frac{1}{2}\mu\left(\frac{\partial u_i}{\partial x_j} + \frac{\partial u_j}{\partial x_i}\right)^2 - \frac{2}{3}\mu\left(\frac{\partial u_k}{\partial x_k}\right)^2\right] \tag{3}$$

where ρ is the fluid density, u_i are the velocity components, p is the pressure, μ is the fluid viscosity, T is the temperature, c_p is the specific heat, k is the thermal conductivity and δ_{ij} is the Kronecker delta function. These equations are non-dimensionalized using the channel hydraulic diameter D_h, reference axial velocity u_r, and reference fluid properties ρ_r, μ_r, $c_{p,r}$, k_r. Pressure is normalized by $\rho_r u_r^2$. All other non-dimensional groups are defined based on these reference properties as follows:

$$Re = \frac{\rho_r u_r D_h}{\mu_r} \qquad Pr = \frac{c_{p,r}\mu_r}{k_r} \qquad Ma^2 = \frac{u_r^2}{\gamma_r R_r T_r} \qquad (4)$$

Based on the kinetic theory of gases, the Mach number can also be expressed as $Ma = ReKn\sqrt{2/\pi\gamma_r}$ where the Knudsen number is defined as $Kn = \lambda/D_h$. For the range of Knudsen and Reynolds numbers considered in this study, the Mach number remains well below 0.3 and therefore, compressibility effects are negligible.

The flow is mass-driven, and the outlet pressure is specified. At the channel inlet, uniform velocity and temperature profiles are specified such that $u = u_{in},\ v = w = 0$ and $T = T_{in}$. When simulating the variable physical property cases, since the inlet pressure is not known a priori, the inlet density is calculated during each iteration and is used to update the inlet velocity for the next iteration. In the case of constant physical properties, the inlet density and velocity will remain constant throughout the solution. The Reynolds number is kept constant while comparing the constant and variable physical property simulations.

A uniform heat flux q'' along with a proper velocity-slip boundary condition is applied at the wall. According to slip flow theory, the slip/jump of the wall is proportional to the velocity and temperature gradients. Velocity-slip and temperature-jump boundary conditions for non-reacting flows can be expressed in a non-dimensional form as [21]:

$$u_s = \frac{5\pi}{16}\left(\frac{2-\sigma_v}{\sigma_v}\right) Kn \left(\frac{\partial u}{\partial n} + \frac{\partial u_n}{\partial x}\right)_w \qquad (5a)$$

$$T_s - T_w = \left(\frac{2-\sigma_T}{\sigma_T}\right)\left(\frac{2\,\gamma}{\gamma+1}\right)\frac{Kn}{Pr}\left(\frac{\partial T}{\partial n}\right)_w \qquad (5b)$$

where T_w is the wall temperature, u_s and T_s are the velocity and temperature of the gas at the wall, u_n is the normal velocity and n is the wall normal direction, and γ is the specific heat ratio. The tangential momentum accommodation coefficient σ_v and energy accommodation coefficient σ_T are equal to zero for specular reflection at the wall and equal to 1 for diffuse reflection [1]. For most engineering applications they are close to unity and considering the approximate nature of the slip theory, they are assumed to be equal to 1 in the present study. Since a constant heat flux is specified at the wall, the temperature-jump boundary condition will only be used for calculating the Nusselt number.

NUMERICAL IMPLEMENTATION

The solution domain is discretized using an orthogonal grid distributed non-uniformly. Grid point density is higher near the walls and channel inlet in order to better resolve the gradients in these regions. Also, since the channel geometry is symmetric, only one quarter of the channel is simulated numerically. A collocated finite-volume code following Rhie and Chow [22] is developed to discretize the governing equations. The Pressure Weighted Interpolation Method is implemented to relate the control volume face velocities to nodal pressure values. Pressure and temperature are assumed to have a linear distribution between adjacent cells. The face advected velocities are approximated using a Linear Deferred Correction scheme to improve the upwind approximation. A restarted Generalized Minimal Residual solver with pre-conditioner is used to solve the system of linear equations [23].

GRID INDEPENDENCE AND VALIDATION

A non-uniform grid with linear expansion is generated in the x, y and z directions. The cross-sectional grid resolution is studied by varying the number of grid points in the y and z directions and comparing flow and heat transfer parameters to the available analytical and numerical results.

Ebert and Sparrow [24] analyzed the velocity and pressure drop effects in rarefied gaseous flows in rectangular ducts and proposed a series solution for the fully-developed velocity distribution of an incompressible constant-property flow within the channel. The fully-developed friction factors at two different aspect ratios are compared to analytical results in Table 1. A good agreement is observed between the numerical simulations and the analytical results.

Table 1: Comparison of no-slip fully-developed friction factor and Nusselt number in rectangular channels with constant wall heat flux

Cross sectional grid		fRe		Nu	
		Present	[24]	Present	[16]
α = 1	10 X 10	13.29	14.22	2.96	3.09
	25 X 25	14.03		3.05	
	30 X 30	14.14		3.07	
α = 2	10 X 20	14.71	15.54	2.92	3.02
	25 X 50	15.40		2.99	
	30 X 60	15.46		3.01	

In order to verify the numerical treatment of the energy equation, the fully developed Nusselt numbers in rectangular channels are also compared to analytical results in Table 1 with $Pr = 0.7$. In these simulations the physical properties are kept constant and the viscous dissipation terms are ignored.

RESULTS AND DISCUSSION

In this section, the effects of compressibility and variable physical properties on the flow and heat transfer characteristics of slip-flow will be presented. Since a large number of variables can change in this type of problem, some parameters are kept constant in order to make a meaningful comparison between the constant property simulations and variable property simulations. To this end, throughout this section the Reynolds number is set equal to 1. The inlet gas temperature in all simulations is assumed to be $T_{in} = 350\,K$. Reference gas temperature is set equal to the inlet temperature and all other reference physical properties of the gas, summarized in Table 2, are calculated at this temperature.

In variable physical property simulations, the stated Knudsen numbers are those at the channel outlet and the

Knudsen number elsewhere is related to temperature and pressure of the gas as [1]:

$$\frac{Kn}{Kn_{out}} = \left(\frac{p_{out}}{p}\right)\left(\frac{T}{T_{out}}\right)^{0.5+\omega} \tag{6}$$

where ω is the viscosity index and can range from 0.6 to 0.9. In the present study, for air as the working fluid, ω is assumed to be equal to 0.7.

Table 2: Hydraulic diameter and the reference physical properties of the gas used in the simulations

Density (kg/m^3)	1.0
Viscosity (Pa s)	2.079×10^{-5}
Conductivity (W/m K)	3.0091×10^{-2}
Constant-pressure specific heat (J/kg K)	1009.35
Specific gas constant (J/kg K)	286.9
Specific heat ratio γ (J/kg K)	1.4
Viscosity index ω	0.7
Prandtl number Pr	0.697
Hydraulic diameter D_h (μm)	10

The equation of state can be utilized to link the density of the gas to its pressure and temperature within the microchannel. Ideal gas assumption is accurate within the ranges of pressure and temperature considered in this study [25]. Viscosity, thermal conductivity and specific heat are determined by the following correlation:

$$\psi = a + bT + cT^2 + dT^3 \tag{7}$$

in which ψ is any of the above-mentioned properties and a, b, c and d are constants given in Table 3 for air. This fitting is accurate for $300K \leq T \leq 1000K$ [26]. For clarity and future reference, the axial variations of non-dimensional viscosity, thermal conductivity and specific heat are shown in Figure 2 as a function of position along a square channel with an outlet Knudsen number of 0.1 at $Re = 1$ and $q'' = 5000\ W/m^2$. Here, $x^+ = x/D_h Re$ is the dimensionless axial position. As observed, the thermal conductivity variation is the highest with about 15% difference between the inlet and outlet. Specific heat, on the other hand, remains very close to the reference inlet value along the channel.

Table 3: Thermophysical property coefficients of air

ψ	μ(Pa s)	k(W/mK)	c_p (J/kgK)
a	2.345×10^{-6}	-4.536×10^{-3}	1013
b	6.203×10^{-8}	1.234×10^{-4}	-0.1571
c	-2.920×10^{-11}	-7.945×10^{-8}	4.910×10^{-4}
d	7.267×10^{-15}	2.728×10^{-11}	-2.055×10^{-7}

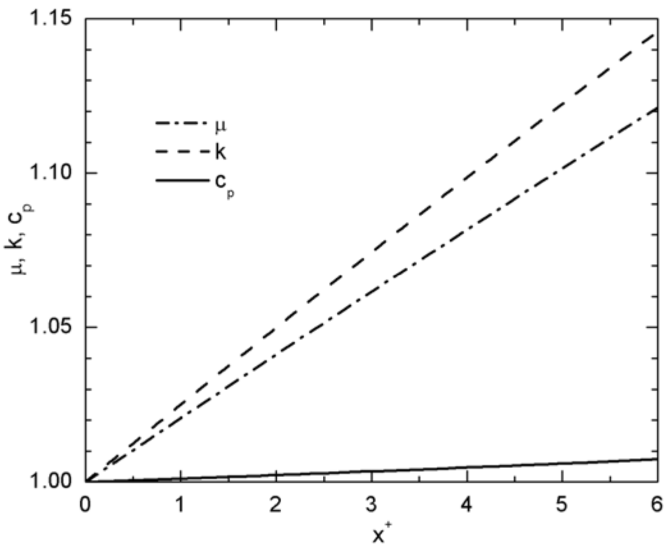

Figure 2: Axial variation of the local Knudsen number and bulk mean temperature along a square channel for $Kn_{out} = 0.1$ at $Re = 1$ and $q'' = 5000\ W/m^2$.

FRICTION FACTOR

For practical engineering purposes, the local friction coefficient $f = 2\tau_w/\rho_{in}u_{in}^2$ in the channel is of key importance. Figure 3 demonstrates the variation of friction coefficient along a square channel for different Knudsen numbers. A wall heat flux of $q'' = 5000\ W/m^2$ is applied peripherally. For the no-slip case, the increase in temperature changes the gas density and viscosity in the developing region gradually and therefore the variable property effects are negligible compared to entrance region effects. After the flow development in the channel, however, increase in gas viscosity and velocity gradients next to the wall cause a noticeable increase in the friction coefficient. In slip-flow, on the other hand, the variable physical property simulations predict a higher friction factor compared to the constant property cases everywhere. This can be attributed to a number of reasons. The change in gas density results in slightly higher velocity gradients in the developing region which will increase the friction coefficient. The variation of the Knudsen number, equation (6), also affects the local friction coefficients. Previous studies have shown that the friction factor is generally higher for lower Knudsen numbers under similar conditions [27]. Since the gas is heating in this case, the ratio of the gas temperature to the outlet temperature is smaller than 1 in every cross section. Therefore, in the slip-flow simulations, the variable-property cases have lower Knudsen numbers as compared to the constant-property simulations. This can be better observed in Figure 4 where the axial distribution of the local Knudsen number is shown for an outlet Knudsen number of 0.1 at $Re = 1$ and $q'' = 5000\ W/m^2$. A lower Knudsen number results in higher friction factors at the inlet. Also a higher gas viscosity next to the wall due to the rising gas temperature results in a higher shear stress. All of these factors contribute to an increase in the friction coefficient in variable-property simulations.

Numerical values suggest that the change in the Knudsen number is the most important factor in increasing the friction coefficient at the inlet where the velocity gradients are considerably large and slip-flow effects are dominant. As the flow field develops in the channel, the result of both simulations become closer to each other up to a point where the constant-property flow fields become fully-developed. From there on, with reduction in slip-flow effects, the gradual increase in the wall temperature steadily increases the gas viscosity, and consequently the friction factor increases at a steady pace as observed in Figure 3.

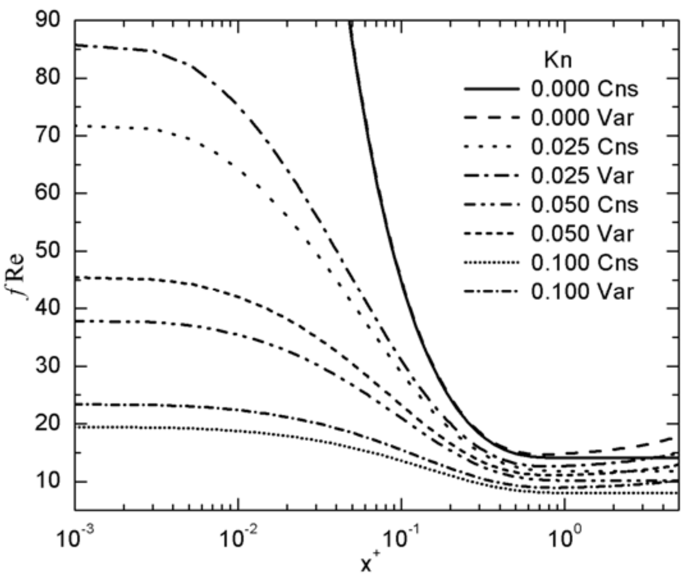

Figure 3: Axial variation of friction factor along a square channel at different outlet Knudsen numbers in constant (Cns) and variable (Var) property simulations with $Re = 1$ and $q'' = 5000\ W/m^2$.

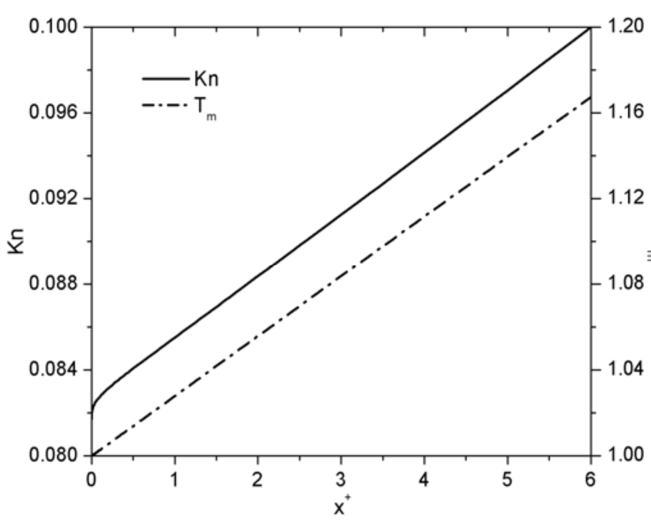

Figure 4: Axial variation of the local Knudsen number and bulk mean temperature along a square channel for an outlet Knudsen number of $Kn_{out} = 0.1$ at $Re = 1$ and $q'' = 5000\ W/m^2$.

The ratio of the friction coefficient of a variable-property simulation to its constant-property counterpart at four different wall heat fluxes is shown in Figure 5 for both no-slip and slip-flow. A wall heat flux of $q'' = -5000$ W/m^2 is also included in order to study the difference between fluid cooling and fluid heating. As observed, in the case of no-slip flows, the friction coefficients remain almost the same up to the point where the flow field in a constant-property simulation becomes fully-developed. Up to that point, the change in the fluid temperature, and therefore physical properties, is small and all cases exhibit almost the same behavior since the axial variation of the friction coefficient is essentially governed by the velocity field development. This is consistent with the behavior observed in Figure 3. However, after this point, the variation in the gas density and viscosity dominates the variation of the friction coefficient. As the wall heat flux becomes stronger, the change in the friction coefficient becomes more apparent. As expected, a higher wall heat flux results in a greater deviation from the constant-property simulation. These observations suggest that the variation of the friction coefficient is negligible in the developing region for the no-slip flow. However in the fully-developed region, depending on the channel length, the friction coefficient variation can become significant as the friction coefficient steadily changes along the channel. Another interesting observation is that when the direction of the wall heat flux is reversed, the results are not symmetric. This can be attributed to the nonlinear nature of property variation as suggested by equation (7).

In the case of slip-flow, however, the developing region exhibits a completely different behavior. Due to the dependence of the Knudsen number on the ratio of the inlet and outlet temperatures (Figure 4), the friction factor ratio in the developing region is affected by the magnitude and direction of the wall heat flux to a greater extent. As discussed earlier, the friction coefficient is higher for lower Knudsen numbers in similar conditions. Therefore, the higher the applied heat flux, the lower the inlet Knudsen number, and consequently a higher friction coefficient. Similar to the no-slip case, different wall heat fluxes follow similar trends with larger discrepancy for stronger heat fluxes. Also, the gas cooling and heating with equal wall heat flux magnitudes do not have symmetrical friction coefficients with respect to constant-property simulations. The nonlinear dependence of the Knudsen number and physical properties on the gas temperature causes this non-symmetrical behavior.

NUSSELT NUMBER

Variable physical properties can alter the temperature field both due to changes in thermal properties and the flow field. Nusselt number variation along the channel provides much insight about the effects of variable properties on the temperature field in general, and on the heat transfer coefficient in particular. The Nusselt number is defined as:

$$Nu = \frac{hD_h}{k_r} = \frac{q''D_h}{k_r(T_m - T_w)} \tag{8}$$

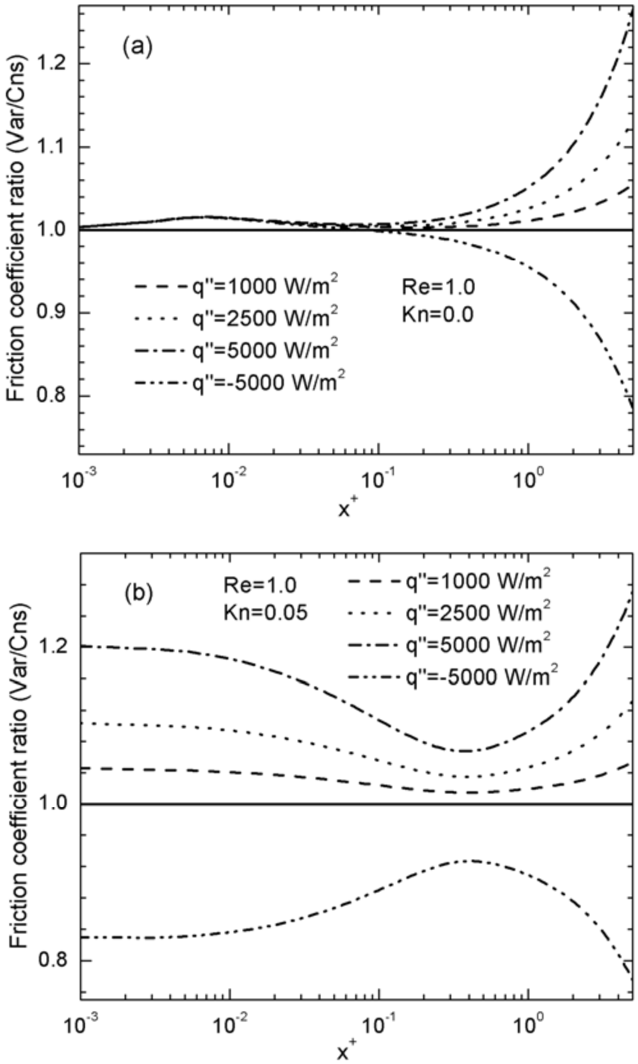

Figure 5: Axial variation of the friction coefficient ratio in a square channel at Re = 1 with different wall heat fluxes for two outlet Knudsen numbers: (a) $Kn = 0.0$ and (b) $Kn = 0.05$

where k_r is the reference conductivity and T_m is the bulk mean temperature defined as:

$$T_m = \frac{\int \rho c_p T \vec{U} \cdot \vec{n}\, dA}{\int \rho c_p \vec{U} \cdot \vec{n}\, dA} \tag{9}$$

In calculating the wall temperature T_w, the temperature-jump boundary condition, equation (5b), is invoked. Axial variation of the bulk mean temperature is shown in Fig. 4 for a sample case with an outlet Knudsen number of 0.1 at $Re = 1$ and $q'' = 5000\ W/m^2$. The linear distribution is due to the applied uniform heat flux and the highly diffusive nature of the problem under consideration.

The Nusselt numbers calculated from constant and variable physical property simulations along the channel are shown in Figure 6 for different Knudsen numbers with a wall heat flux of $q'' = 5000\, W/m^2$ with $x^* = x/D_h RePr$ being the non-dimensional axial position. As observed, the Nusselt number in the developing region is not affected by property changes and is very close to the constant-property simulation for all Knudsen numbers. This is mainly due to the fact that although density and velocity are changing in variable-property simulations, the mass flow rate which is responsible for enthalpy transport is still constant. And since in the developing region, the rise in temperature is small, conductivity and specific heat changes are minimal and the heat transfer coefficient is mainly affected by the temperature field development.

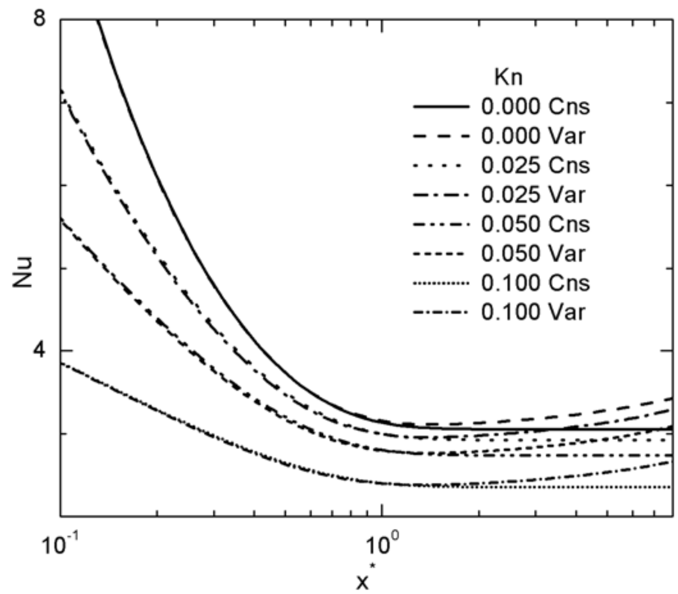

Figure 6: Axial variation of Nusselt number along a square channel for different outlet Knudsen numbers in constant (Cns) and variable (Var) physical property simulations at $Re = 1$

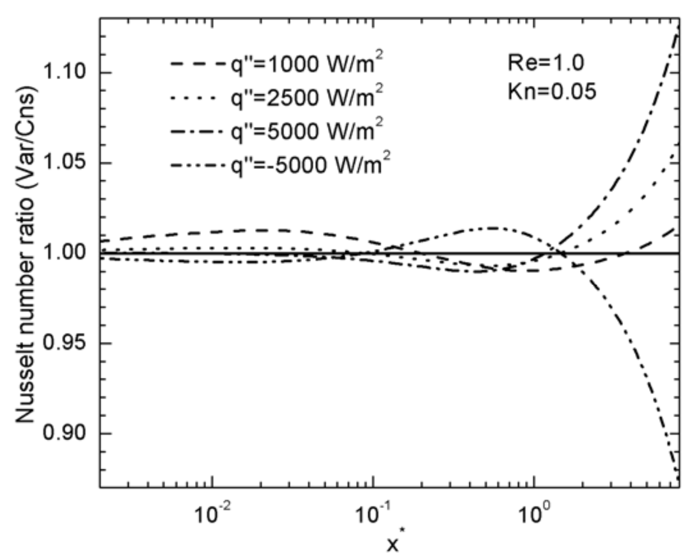

Figure 7: Axial variation of the Nusselt number ratio in a square channel with different wall heat fluxes for an outlet $Kn = 0.05$

It should also be noted that unlike the case of the friction coefficient at the inlet, the variation in Knudsen number in variable-property simulations does not have a direct effect on the temperature field with a constant wall heat flux boundary condition. Therefore, the Nusselt number in the developing region is very similar in both types of simulations. After the development region however, the change in properties of the gas dominates the axial variation of the Nusselt number. In the present case, since the conductivity of air increases with rising gas temperature, the Nusselt number increases along the channel.

In order to study the variable property effects on the Nusselt number variation along the channel more closely, the ratio of the variable-property Nusselt number simulations to their constant-property counterparts are compared to each other in Figure 7, where different wall heat fluxes are considered for the case of $Kn = 0.05$. A negative wall heat flux is also included to study the effect of fluid cooling on the Nusselt number behavior. These results again confirm the weak dependence of the entrance region Nusselt number on variable properties. As observed, the Nusselt number remains fairly close to constant property simulations for different boundary values up to a point where the constant-property simulation becomes fully-developed. At this point, where entrance region effects have diminished and the gas temperature has considerably increased, the rise in gas conductivity begins to play the key role in determining the Nusselt number behavior. The Nusselt number corresponding to all three positive wall heat fluxes follow similar trends with a small decrease in their value right before the entrance length and a steady increase afterwards. Interestingly, the Nusselt number in the cooling case follows the same trend as the heating case symmetrically. The numerical values of the relative increase or decrease in Nusselt number are close to each other in the gas heating and gas cooling cases, respectively.

CONCLUSION

The effects of variable physical properties on the flow and heat transfer characteristics of gaseous slip-flow in microchannels with constant wall heat flux have been studied numerically. Different Knudsen numbers and wall heat fluxes are considered. A co-located finite volume method is used to solve the governing transport equations simultaneously with proper slip/jump boundary conditions at the walls.

A large number of parameters vary as the temperature changes, and therefore, the friction coefficient and Nusselt number values deviate from the constant property simulations. Variable physical properties can change the flow and heat transfer characteristics in both the entrance and fully-developed regions. The friction coefficient behavior in the entrance region of no-slip flows is mostly dominated by the flow field development; that is, physical property variations have a minimal effect. However in this region, the slip-flow friction coefficient is affected by property changes mainly due to the dependence of the Knudsen number on temperature. In the fully-developed region, the constant property assumption under predicts the friction coefficients in the case of gas heating and over predicts them in the gas cooling scenario. Also, if the direction of the heat flux is reversed, the friction coefficient does not change symmetrically due to the nonlinear dependence of the physical properties and Knudsen number on the gas temperature.

Nusselt numbers in the developing region do not change noticeably due to property variations for any Knudsen number. Contrary to friction coefficient variation of slip-flow, since the boundary condition is not a function of the Knudsen number, the heat transfer coefficient is mainly governed by the temperature field development in the entrance region. As the gas temperature increases along the channel, gas conductivity variation starts playing the dominant role in determining the Nusselt number behavior in the fully-developed region.

ACKNOWLEDGEMENT

This study is financially supported by the Natural Sciences and Engineering Research Council of Canada.

REFERENCES

[1] Kennard, E. H., 1938. Kinetic Theory of Gases, McGraw-Hill, New York.

[2] Harley, J. C., Huand, Y., Bau, H., Zemel, J. N., 1995. Gas flow in microchannels. J. Fluid Mech. 284, 257-274.

[3] Arkilic, E. B., Schmidt, M. A., Breuer, K. S., 1997. Gaseous slip flow in long microchannels. J. MicroElectroMechanical Syst. 6, 167-178.

[4] Morini, G. L., Spiga, M., 1998. Slip flow in rectangular microtubes. Microscale Thermophys. Eng. 2, 273-282.

[5] Beskok, A., 1999. A model for flows in channels, pipes, and ducts at micro and nano-scale. Microscale Thermophys. Eng. 3, 43-77.

[6] Meinhart, C. D., Wereley, S. T., Santiago, J. G., 1999. PIV measurements of a microchannel flow. Exp. in Fluids 27, 414-419.

[7] Morini, G. L., Spiga, M., Tartarini, P., 2004. The rarefaction effects on the friction factor of gas flow in microchannels. Superlattices Microstruct. 35, 587-599.

[8] Hsieh, S. S., Tsai, H. H., Lin, C. Y., Huang, C. F., Chien, C. M., 2004. Gas flow in a long microchannel. Int. J. Heat Mass Transf. 47, 3877-3887.

[9] Morini, G. L., 2004. Single-phase convective heat transfer in microchannels: a review of experimental results. Int. J. Therm. Sci. 43, 631-651.

[10] Chen, C., 2004. Numerical method for predicting three-dimensional steady compressible flow in long microchannels. J. Micromech. Microeng. 14, 1091-1100.

[11] Van Rij, J., Harman, T., Ameel, T., 2007. The effect of creep flow on two-dimensional isoflux microchannels. Int. J. Therm. Sci. 46, 1095-1103.

[12] Liu, J.T., Peng, X.F., Wang, B.X., 2008. Variable-property effect on liquid flow and heat transfer in microchannels. Chem. Eng. J. 141, 346-353.

[13] Hooman, K., Ejlali, A., 2010. Effects of viscous heating, fluid property variation, velocity slip, and temperature jump on convection through parallel plate and circular microchannels. Int. Comm. Heat Mass Transf. 37, 34-38.

[14] Gulhane, N. P., Mahulikar, S. P., 2010. Numerical study of compressible convective heat transfer with variations in all fluid properties. Int. J. Therm. Sci. 49, 786-796.
[15] Rostami, A.A., Saniei, N., Mujumdar, A.S., 2000. Liquid flow and heat transfer in microchannels: A review. Heat Technol. 18, 59–68.
[16] Yu, S., Ameel, T. A., 2002. Slip flow convection in isoflux rectangular microchannels. J. Heat Transf. 124, 346-355.
[17] Kuddusi, L., Ceten, E., 2007. Prediction of temperature distribution and Nusselt number in rectangular microchannels at wall slip condition for all versions of constant heat flux. Int. J. Heat Fluid Flow 28, 777-786.
[18] Nonino, C., Del Giudice, S., Savino, S., 2007. Temperature-dependent viscosity and viscous dissipation effects in simultaneously developing flows in microchannels with convective boundary conditions. J. Heat Transf. 129, 1187-1194.
[19] Van Rij, J., Ameel, T., Harman, T., 2009. The effect of viscous dissipation and rarefaction on rectangular microchannel convective heat transfer. Int. J. Therm. Sci. 48, 271-281.
[20] Van Rij, J., Ameel, T., Harman, T., 2009b. An evaluation of secondary effects on microchannel frictional and convective heat transfer characteristics. Int. J. Heat Mass Transf. 52, 2792-2801.
[21] Qazi Zade, A., Renksizbulut, M., Friedman, J., 2008. Slip/jump boundary conditions for rarefied reacting/non-reacting multi-component gaseous flows. Int. J. Heat Mass Trans. 51, 5063-5071.
[22] Rhie, M. C., Chow, W. L., 1983. Numerical Study of the Turbulent Flow Past an Airfoil with Trailing Edge Separation. AIAA Journal 43, 357-372.
[23] Saad, Y., Schultz, M.H., 1986. GMRES: A generalized minimal residual algorithm for solving nonsymmetric linear systems. SIAM J. Sci. Stat. Comput. 7, 856-869.
[24] Ebert, W. A., Sparrow, E. M., 1965. Slip flow in rectangular and annular ducts. J. Basic Eng., Trans. ASME, 1018-1024.
[25] Karniadakis, G., Beskok, A., Aluru, N., 2005. Microflows and Nanoflows: Fundamental and Simulation, Springer, New York.
[26] Reid, R. C., Prausnitz, J. M., Sherwood, T. K., 1977. The properties of gases and liquids, third ed. McGraw-Hill, New York.
[27] Renksizbulut, M., Niazmand, H., Tercan, G., 2006. Slip-flow and heat transfer in rectangular microchannels with constant wall temperature. Int. J. Therm. Sci. 45, 870-881.